Oil Shale, 2005, Vol. 22, No. 3
pp. 291-303
ISSN 0208-189X

https://doi.org/10.3176/oil.2005.3.04

ATOMISTIC MOLECULAR SIMULATION OF THERMAL VOLUME EXPANSION OF ESTONIAN KUKERSITE KEROGEN

T. KAEVAND[(a)], Ü. LILLE[*(b)]

[(a)] Chair of Information Technology, Estonian Business School
3 Lauteri Str., Tallinn,10114 Estonia

[(b)] Department of Chemistry, Tallinn University of Technology
15 Akadeemia Rd., Tallinn, 12618 Estonia

Thermal volume expansion of Estonian kukersite kerogen was simulated with the aim to predict the response of kerogen to thermal stress in laboratory and geological conditions. The simulation was performed using a general amber force field evaluated by the calculation of non-polar cohesive energy density based on atomic interactions and value of corresponding solubility parameter. At constant pressure in the range 1–1,000 bars the specific volume vs. temperature plots were registered, and two linear regions at 150–525 and 550–900 K (at the pressure one bar) were identified. In the gap between these regions a changeover point, termed as apparent second-order polymer-like phase transition from the glassy to the rubbery state, is located. At higher pressures the changeover shifts to higher temperatures. Its possible meaning in kerogen transformations at retorting and geological conditions is discussed. A further experimental study of the observed phenomenon is needed.

Introduction

Interest in the research of kerogens, which are organic recalcitrant, cross-linked and mostly glassy geopolymers, is based on the desire to understand diagenetic and possible industrial processes aimed mainly at the transformation of kerogens as the organic component of oil shales into low- molecular mass compounds. These processes are thermal or microbiological [1–5]. In both cases a key role is played by the molecular mobility and the amorphous structure of kerogens based on the complex interplay of covalent and non-bonded interaction. Particularly the nature of the latter interactions and the role they play in kerogens is badly understood so far in comparison to that of synthetic linear polymers.

[*] Corresponding author: e-mail address *lille@chemnet.ee*

The intensity of non-covalent interactions depends on the phase of a solid polymer, i.e. distinct arrangement of atoms, molecules and particles associated with them. In a solid polymer glassy and (or) rubbery phases are observed. The transition from the glassy to the rubbery phase is not associated with the latent heat and is termed as the second-order phase transition. In the rubbery phase the density of the non-bonded interactions and the stiffness and viscosity of the material are *ca* thousand times less than in the glassy phase [6]. Therefore, phase transition is a tool to change the molecular mobility and the related properties effectively. It is remarkable that the molecular relaxation time, i.e. the structural-rearrangement response time, varies enormously with temperature and covers the time-span from geological times in the glassy phase to ps order in the liquid [7].

Besides laboratory experimental methods atomistic molecular simulation has been widely used for identification and exploration of phase transitions in amorphous polymers [8–13]. Simulation in NPT[1] conditions enables to generate specific volume (or its reciprocal value, i.e. density) *vs*. temperature curves analogously to these of dilatometric methods. The slope of this plot is determined by the volume coefficient of expansion, the related thermodynamic variable, the first derivative of volume. The change in the slope is caused by the increase in thermal capacity and denotes glass transition temperature (T_g). In spite of different time scales of molecular-dynamical (MD) simulations and laboratory dilatometric experiments, the results of both methods coincide in general.

Hopefully the study of volume expansion of kerogens will yield new insights into their polymeric nature and the role of non-bonded interactions. This article presents our results of the study of thermal expansion of Estonian kukersite kerogen (further kerogen if not specified otherwise) and is the continuation of our efforts to simulate the properties of this geopolymer [14, 15].

Methodology of the Calculations

In the molecular simulation of polymer glasses much attention is paid to the generation of well-relaxed disordered glass structures at realistic densities ([9] and references therein). Due to the complex nature of geomacromolecules, like kerogen, the developed generation techniques are not directly transferable to the kerogen simulation. However, the general features can be followed, i.e. the preparation of the isolated molecule using a proper force field, generation of the initial bulk (glass) phase and its relaxation.

[1] Here and below the following designations are used: N – number of particles, P – pressure, T – temperature, V – volume.

Preparation of an Isolated Gas-Phase Kerogen Molecule

As input the hin file of kerogen conformer IVA in the gas phase obtained in our previous work [15] and based on MD and molecular-mechanical (MM) calculations of a 2-dimensional kerogen compositional structural model ($C_{420}H_{634}O_{44}S_4NCl$, molecular mass M = 6562 amu, [16]) in MM+ force field was used. From this file the initial isolated gas-phase structure was generated using Antechamber and Leap subprograms of the molecular simulations package AMBER 7 (based on the general amber force field, GAFF [17]). This structure does not contain hydrogen bonds (see below). Further calculations were carried out using subprogram SANDER from the same packet (time step 0.4 fs and cutoff 8.5 Å).

The initially generated structure was energy minimized (E_{tot} = = 422 kcal/mol), and thereafter various NVT runs were performed. The best local minimum was obtained using a 80 ps MD run at 300 K, followed by cooling (20 ps) and minimization. This procedure provided one starting configuration for subsequent processing. The other five starting configurations were generated from this one by running MD and selecting configurations at intervals of 5 ps. In this way, six isolated gas-phase kerogen model conformers with minimum energy were generated (Table 1).

Table 1. **Total Energy (E_{tot}) and Energy of van der Waals Interactions (E_{VdW}) of Model Conformers in the Gas and in the Bulk Phase (kcal/mol)**

Conformer	Gas phase		Bulk phase	
	E_{tot}	$-E_{VdW}$	E_{tot}	$-E_{VdW}$
1	391	166	193	462
2	394	165	170	470
3	402	157	259	448
4	399	160	218	446
5	394	163	186	469
6	401	166	217	455
Average (± standard deviation)	397(± 4.4)	163 (± 3.7)	207(± 31)	458 (±10)

Preparation of the Real-Density Initial Bulk (Glassy) Phase and Its Relaxation

The bulk phase was created using periodic boundary conditions. First, a MD run was accomplished in NVT conditions in order to bring the system to 300 K and compressed at 10^4 Pa (NTP ensemble) to obtain the real density $d = 1.11$ g/cm^3 [18]. The obtained high-energy system was then equilibrated in NVT conditions at 1000 K during 20 ps followed by stepwise cooling (10 steps of 100 K each followed by 8 ps for equilibration) and energy minimization to obtain the glass structure in a box with dimensions 3×21.2 Å. Stepwise cooling is necessary to obtain the bulk phase with

minimum value of total energy. The other bulk-phase structures were generated analogously (see Table 1).

We can notice that the high temperatures and pressures used are necessary to give the system enough energy to overcome the energy barriers between local minima, to get more data points on the regression lines (see below), and to obtain the real macroscopic density. Classical force fields do not contain any terms for breaking the covalent bonds, and the pressure is related to the virial calculated as the product of the positions of atoms and the derivative of the potential energy function derived from the force field used [19].

Simulation of Thermal Volume Expansion

The molecular system corresponding to conformer 1 was modeled as the NTP ensemble using the general procedure described in [13] (and references therein). By using a 20-ps MD run in NVT conditions the system was carried to 150 K and then heated analogously in steps per 25 K to higher temperatures up to 900–950 K. At each temperature and pressures of 1, 500, and 1000 bar, the simulation was performed in NTP conditions during 100 ps. The density of the system was saved at each 50 time steps. The final density at each temperature is the average value of the last 12,500 steps of the simulation. Regression analysis of the obtained specific volume (reciprocal of density) *vs*. temperature plots was performed using Excel3 software (confidence level 0.95). The optimal linear regions were determined and checked using an assumption that the changeover point lies between these regions [20]. The volume coefficients of expansion (α_G and α_R in the glass and rubbery state, respectively) were calculated as $[(Vs_2 - Vs_1)/Vs_1]/T_2 - T_1$, where Vs is specific volume (further volume if not specified otherwise), the subscripts 1 and 2 denote the borders of the linear region of the regression line (see below).

The total time of the simulation over the temperature interval 150–950 K was 3.4 ns. Calculations were performed using computer cluster of Institute of Cybernetics at Tallinn University of Technology.

Results and Discussion

Validation of the Initial Model

Cohesive energy density and the value of the solubility parameter have often been calculated to check the suitability of the force field and the methodology of the glass generation used.

Cohesive energy characterizes the strength of intermolecular forces in the bulk phase. This value (equal to 295 ± 13.7 kcal/mol) for the generated kerogen model was obtained as the energy difference of non-bonded interactions in the isolated molecule and in the molecule in the bulk phase

(see Table 1). Taking into account the molar volume corrected for thermal expansion it resulted in the cohesive energy density 54.4 ± 2.5 cal/cm^3. Square root of this value corresponds to the dispersion component δ_D of the solubility parameter equal to 7.4 ± 0.2 (cal/cm^3)$^{1/2}$ at 0 K. The range of the real values of the total solubility parameter δ_T of various I–II type kerogens has been estimated from the results of swelling experiments in organic solvents with known parameter values, and it comprises *ca* 9–10 (cal/cm^3)$^{1/2}$ [21, 22]. The experimental value for the kerogen under discussion has not been determined so far, but one can conclude that the difference between the calculated δ_D and expected experimental δ_T value is mainly caused by the negligence of polar and hydrogen-bonding components and is consistent with the results of such calculations for polymers [23]. Therefore the force field used is acceptable at this stage of the research.

In the context of kerogen research, the value of the solubility parameter has a significant meaning characterizing swelling ability of kerogen in various solvents (see below) and the expelling efficiency of the generated petroleum [22].

Simulation of the Thermal Volume Expansion

Registration of volume *vs*. time curves at various temperatures showed that the volume fluctuations reach a stable equilibrium level already at about 30 ps (Fig. 1). Therefore the observed volume *vs*. temperature curves show the equilibrium volume values at each temperature.

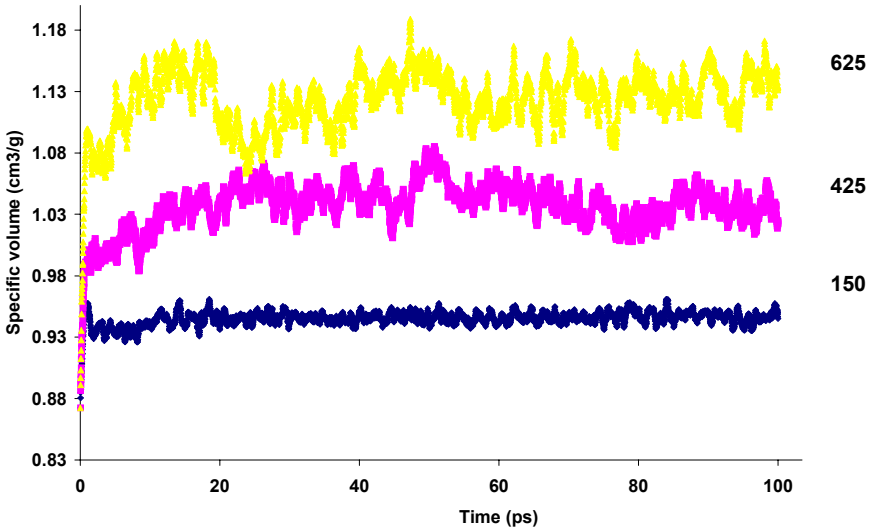

Fig.1. Specific volume *vs*. time at 150, 425 and 625 K in NPT conditions at the pressure 1 bar

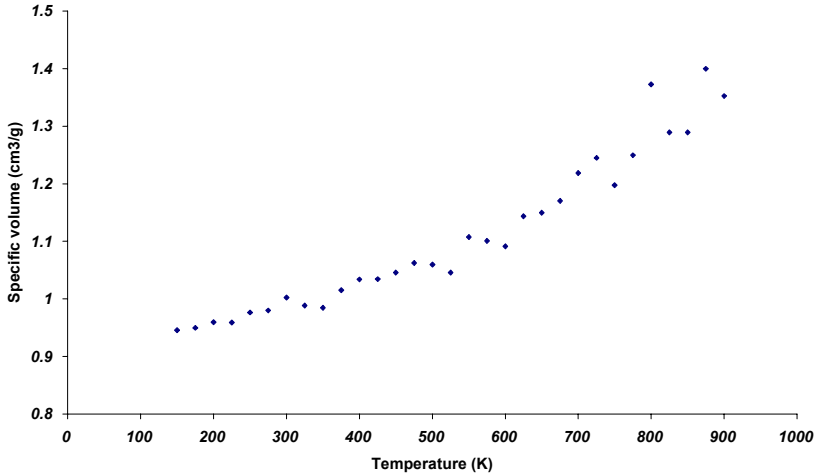

Fig. 2. Specific volume *vs*. temperature in NPT conditions at the pressure 1 bar

Visual inspection of the volume *vs*. temperature plot (Fig. 2) at the pressure 1 bar shows larger scattering of data in comparison to that observed in the simulations of linear polymers, e.g. [13]. Between 500 and 600 K a broad "elbow" can be seen. Based on the assumption mentioned above, one can identify two linear regions on this plot. In the first region, 150–525 K, the value of the expansion coefficient corresponds to that of glassy amorphous polymers [6], and the glassy kerogen as an amorphous solid expands mainly due to the vibrations of atoms. The second region, 550–900 K, is characterized by an approximately twice higher slope of the regression line, i.e. by the higher value of expansion coefficient (and higher dispersion).

In the polymer science such a change in the slope is characteristic to the onset of phase transition to the viscoelastic region, i.e. into rubbery state. In this state larger molecular segments are involved in the motions pointing to the cleavage of physical cross-links. The role of these cross-links is reflected in the swelling ability of kerogens, in general comprising up to *ca* 50% volume in organic solvents [21].

The second region obviously corresponds to the rubbery state. The temperature span of the overlapping region, 500–600 K, where the phase transition probably takes place, is somewhat wider than that of synthetic polymers (*ca* 20–30 degrees). This is consistent with data from the polymer science showing that the glass-rubber transition becomes broader and less distinct as the concentration of cross-links increases [24]. Keeping in mind the complex structure of the kerogen unit model in comparison to the model of synthetic linear polymers, the identification of the shown "elbow" on the volume *vs*. temperature plot is noteworthy because amorphous polymers often exhibit more than one transition, and the glass-rubber transition could be partly masked by secondary transitions [25].

Here it is necessary to point at the results obtained in the study of Rundle kerogen [26]. Observation of ^{1}H n.m.r. transients decaying exponentially (rapidly and slowly) (in the time scale of *ca* 10^{-5} s) enables to identify the corresponding glass-rubber transitions: the first very broad one occurs from below room temperature to *ca* 500 K, and the second one at 600–680 K overlapping the decomposition of the bulk kerogen.

The intersection of the regression fits enables to estimate the value of apparent T_g as 540 K. At pressures 500 and 1000 bars the T_g value is shifted to 558 and 605 K, respectively. This shift is *ca* twice as large as that observed in the case of linear polymers. The shape of the plots and the dispersion are similar to these observed at 1 bar, but, due to the decrease in the free volume, the curvature flattens with the increasing pressure.

Summary results of the statistical analysis of the scatter plots are shown in Table 2. From the given data the following conclusions can be drawn:

1) The identification of the changeover point on the scattering plots is statistically acceptable (compare the s_Y values in the corresponding temperature ranges). Considering the high values of correlation coefficient in the total temperature range one has to keep in mind that a straight line can be used to approximate almost any curved line if the interval of population is restricted sufficiently [27], i.e. at the relatively small number of observations like in our case,
2) The standard deviation of the calculated T_g values as estimated from the intersection of the upper/lower and lower/upper deviation belts of the regression lines, respectively, comprises *ca* 100 K. This is caused by large errors of the regression line parameters, particularly of the second linear region. As repeated runs give nearly the same result, there probably exist molecular reasons which we cannot identify at this stage of work.

The calculated T_g value at the pressure of 1 bar exceeds that of amorphous polymers by at least 100 degrees, e.g. the T_g values of polystyrene and thermoset epoxyresins with varying content of hardener are 373 [6] and 365–410 K [28], respectively, that of polyvinyl phenol is 445 K [13]. However, the high T_g value of kerogen (and its brittleness) in comparison to that of man-made polymers is quite logical, and it can be attributed to gelation and vitrification processes during geological times.

Here it is necessary to elucidate the possible role of hydrogen bonds ignored in our calculation. An about 75-K increase in the T_g value of polyvinyl phenol in comparison to that of polystyrene is caused by a rather extensive network of hydrogen bonds in the polyvinyl phenol. The number of potential H-bond donors per one carbon atom in the latter molecule exceeds that of kerogen *ca* three times, whereas the percentage of donors involved in the H-bonds is almost equal [15]. Therefore, the disregard of hydrogen bonds in the kerogen can cause a *ca* 25 K underestimation of its T_g value, which is probably balanced by the difference between the experimental and simulation heating rates reaching 20 K [11].

Table 2. **Results of the Statistical Analysis of the Scatter Plots**

Item	Descriptor	Pressure, bars								
		1			500			1,000		
1	T range, K	150–525	550–900	150–900	150–550	575–900	150–900	150–575	600–950	150–950
2	n	16	15	31	17	14	31	18	15	33
3	R^2	0.936	0.877	0.912	0.944	0.952	0.956	0.926	0.911	0.961
4	$s_Y \times 10^{-2}$	1.05	3.65	3.91	0.910	1.45	2.09	1.11	1.73	1.79
5	P	9.49×10^{-10}	2.70×10^{-7}	2.20×10^{-17}	8.98×10^{-11}	2.79×10^{-9}	3.46×10^{-21}	1.85×10^{-10}	3.47×10^{-8}	2.10×10^{-23}
6	$b_1 \times 10^{-4}$	3. 26	8.41	5.70	2.86	5.92	4.21	2.84	4.74	3.61
7	$s_{b1} \times 10^{-5}$	0.228	8.72	3.14	1.80	3.84	1.68	2.01	4.12	1.31
8	b_0	0.892	0.615	0.811	0.890	0.719	0.844	0.873	0.758	0.845
9	$s_{b0} \times 10^{-2}$	0.813	6.39	1.79	0.668	2.86	0.959	0.774	3.23	0.782
10	$\alpha \times 10^{-4}$ K^{-1}	3.46	7.80	6.36	3.06	5.59	4.64	3.10	4.55	4.01
11	s_α	0.630	2.20	1.44	0.518	0.916	0.722	0.606	1.02	0.576
12	T_g, K	540		–	558		–	605*		–
13	s_{Tg}	90		–	80		–	130		–

Items: n – number of data points; R^2 – squared correlation coefficient; s – standard deviation; Y – predicted ordinate value of the line of best fit; P – probability of the significance; b_1 – slope; b_0 - intercept; α – thermal volume expansion coefficient; T_g – changeover point.

* The best choice of linear regions.

The observed estimates of volume expansion coefficients in the glassy and rubbery phases and the phase transition temperature at the pressure 1 bar (see Table 2, item 10) give 0.08–0.4 as the hypothetical fractional free volume value for kerogen, which is *ca* twice as high as the value of linear polymers calculated by the general empirical relationship:

$$(\alpha_R - \alpha_G)\, T_g = \text{constant} = 0.113$$

where the constant 0.113 shows the fractional free volume in the polymer [6]. However, the lower limit of the observed estimate for kerogen includes the realistic value. Note that the low value of fractional free volume reflects high brittleness of the material.

The range of T_g value does not contradict the known data of the thermal behavior of kerogen. At heating kerogen at 523 K during up to 768 h pronounced changes were observed in the absorption at 3200–3300 and 1600 cm^{-1} [29]. At 550 K kerogen undergoes thermal degradation yielding volatiles and pyrobitumen (at 456-h heating, 9 and 18%, respectively) [30]. According to differential thermal analysis data intensive degradation begins at *ca* 575 K [31]. As molecular motions in the phase transition region are quick processes in comparison to thermal cleavage, the phase transition obviously precedes the latter process.

The shrinkage of oil shales during kerogen degradation [32] may be caused by the preceding phase transition of kerogen. However, shrinkage after kerogen decomposition is of course a quite different phenomenon.

According to these considerations the calculated T_g values are in line with known properties of kerogen.

Below we speculate on the possible role of phase transition in geological conditions considering kerogen studied in this report a representative of marine kerogens. In accordance with the Arrhenius-type time-temperature dependence, the transformation of kerogens into oil starts in general already at *ca* 325 K [3], i.e. *ca* 200 K below the T_g value of kerogen. When the temperature of the polymer is *ca* 50 degrees below of its T_g value, then the relaxation time of molecular motions caused by thermal stress is practically infinite, because these motions obey the viscosity-like time-temperature dependence (Vogel–Fulcher–Tamman equation [25]). From this point of view the cleavage of covalent bonds should be the necessary first step in the pyrobitumen formation in geological conditions. Of course, the possible presence of a liquid phase and the influence of inorganic matrix cannot be ignored.

Biodegradation and weathering of sedimentary organic matter are processes depending on the viscosity and brittleness (related to erosion) i.e. properties determined by the molecular mobility and the presence of oxygen [33, 34]. The estimate of the lowest value of T_g of kerogen 450 K (we ignore here the effect of the pressure) remains 100 degrees higher than the maximum boundary for life in the deep nutrient-depleted Earth estimated

equal to 350 K [4]. This is consistent with an extremely high resistance of kerogen towards microbial attacks. Figuratively speaking kerogen is "locked" at the temperatures *ca* 50 degrees below T_g. However, there is some evidence that the microorganisms are able to use ancient organic matter [5, 35, 36]. When interpreting these results it is necessary to keep in mind the phase of the concrete kerogen, because low-density cross-linked kerogens can comprise a rubbery phase at temperatures as low as 300 K [37].

The general lability of many kerogens in oxidizing medium including oxygen-rich surface waters is logical because the action of low-molecular mass oxidative particles is obviously not controlled directly by the molecular mobility of kerogens.

In general, our model, based on a certain analogy between the structure of kerogen and that of synthetic thermosets representing a huge macromolecule whose size is confined only by the boundaries of the reaction vessel, helps to shed some light upon essential aspects of kerogen behavior at retorting and in geological conditions. However, the nature of the kink on the volume *vs*. temperature plot of kerogen, termed here as the apparent polymer-like phase transition, should be studied using ^{1}H n.m.r. spectroscopy and selective labeling of groups in kerogen.

The change in the T_g value caused by the presence of organic solvents is the subject of further simulations.

Conclusions

Using the atomistic molecular mechanical simulation of thermal volume expansion of kerogen, the presence of a changeover point on the specific volume *vs*. temperature plot has been shown. Based on thermal and recalcitrant properties of kerogen, this point has been putatively interpreted as the second-order phase transition. Laboratory experimental work is needed to elucidate the nature of the observed phenomenon.

Acknowledgements

The corresponding author is grateful to the Estonian Science Foundation for financial support (Grant No. 5624), to Dr. Omar Parve and Prof. Jüri Soone for the possibility of co-operation with the target-financed themes, and to Prof. Mati Karelson for customizing computational programmes.

REFERENCES

1. *Lewan, M. D.* Experiments on the role of water in petroleum formation // Geochimica et Cosmochimica Acta. 1997. Vol. 61, No. 17. P. 3691–3723.
2. *Vandenbroucke, M., Behar, F., Rudkiewicz, J. L.* Kinetic modelling of petroleum formation and cracking: implications from the high pressure/high temperature Elgin Field (UK, North Sea) // Org. Geochem. 1999. Vol. 30. P. 1102–1125.
3. *Seewald, J. S.* Organic-inorganic interactions in petroleum-producing sedimentary basins // Nature. 2003. Vol. 426, No. 20. P. 327–333.
4. *Head, I. M., Jones, M., Larter, S. R.* Biological activity in the deep subsurface and the origin of heavy oil // Nature. 2003. Vol. 426, No. 20. P. 344–351.
5. *Aislabie, J.* Biotechnology of oil shale // Proceedings of the Sixth Australian Workshop on Oil Shale. 1991. P. 213–218.
6. *Sperling, L. H.* Introduction to Physical Polymer Science. – Wiley Interscience, New York, Chicester,Weinheim, Brisbane, Singapore, Toronto 2001. P. 296–362.
7. *Zallen, R.* The Physics of Amorphous Solids. – John Wiley Sons, Inc., New York, Chicester, Weinheim, Brisbane, Singapore, Toronto 1998. P. 1–23.
8. *Li, J., Mattice, W. L.* Atom-based modeling of amorphous 1,4-cis polybutadiene // Macromolecules. 1992. Vol. 25. P 4942–4947.
9. *Khare, R., Paulaitis, M. E.* Generation of glass structures for molecular simulation of polymers containing large monomer units: application to polystyrene // Macromolecules. 1993. Vol. 26. P. 7203–7209.
10. *Kim, E.-G., Misra, S., Mattice, W. L.* Atomistic models for amorphous polybutadienes. 2. Poly(1,4-trans-butadiene), poly(1,2-butadiene), and a random copolymer of 1,4-trans-butadiene, 1,4-cis-butadiene, and 1,2-butadiene. // Macromolecules. 1993. Vol. 26. P. 3424–3431.
11. *Han, J., Gee, R. H., Boyd, R. H.* Glass transition temperatures of polymers from molecular dynamics simulations // Macromolecules. 1994. Vol. 27. P. 7781–7784.
12. *Rigby, D., Sun, H., Eichinger, B. E.* Computer simulation of poly(ethylene oxide): force field, PVT diagram and cyclization behaviour // Polymer International. 1997. Vol. 44. P. 311–330.
13. *Gestoso, P., Brisson, J.* Effect of hydrogen bonds on the amorphous phase of a polymer as determined by atomistic molecular modelling // Computational and Theoretical Polymer Science. 2001. Vol. 11. P. 263–271.
14. *Lille, Ü.* Effect of water on the hydrogen bond formation in Estonian kukersite kerogen as revealed by molecular modelling // Fuel. 2004. Vol. 83. P. 1267.
15. *Lille, Ü.* Behavior of Estonian kukersite kerogen in molecular mechanical force field // Oil Shale. 2004. Vol. 21, No. 2. P. 99–114.
16. *Lille, Ü., Heinmaa, I., Pehk, T.* Molecular model of Estonian kukersite kerogen as evaluated by 13C MAS NMR spectroscopy // Fuel. 2003. Vol. 82. P. 799–804.

17. *Case, T. A., Pearlman, D. A., Caldwell, J. W., Ross, W. S., Simmerling, T. A., Darden, T. A., Merz, K. M., Stanton, R. W., Cheng, A. I., Vincent, J. J., Crowley, M., Tsui, V., Gohlke, H., Radmer, R. J., Duan, Y., Pitera, J., Massova, I., Seibel, G. L., Singh, U. C., Weiner, P. K., Kollmann, P. A.* Amber Version 7. Users' Manual, University of California, San Francisco 2002.
18. *Rudin, M. G., Serebrjannikov, N. D.* Handbook of Oil Shale Refiner. – Khimiya, Leningrad, 1988. P. 34 [in Russian].
19. *Leach, A. R.* Molecular Modelling. Principles and applications. – Pearson Education, Harlow, England, 2001. P. 353.
20. *Carter, K. N., Scott, D. M., Salmon, J. K., Zarcone, G. S.* Confidence limits for the abscissa of intersection of two least squares lines such as linear segmental titration curves // Anal. Chem. 1991. Vol. 63. P. 1270–1278.
21. *Larsen, J. W., Parikh, H., Michels, M.* Changes in cross-link density of Paris Basin Toarcian kerogen during maturation // Org. Geoshem. 2002. Vol. 33. P. 1143–1152.
22. *Ritter, U.* Solubility of petroleum compounds in kerogen: implications for petroleum expulsion // Org. Geochem. 2003. Vol. 34. P. 319–326.
23. *Zhao, L., Choi, P.* Study of the correctness of the solubility parameters obtained from indirect methods by molecular dynamics simulation // Polymer. 2004. Vol. 45, No. 4. P. 1349–1356.
24. *Williams, R. J. J.* Transition during network formation // Polymer Networks. Principles of Their Formation, Structure and Properties / R. F. T. Stepto (ed.), Blackie Academic Professional. London, Weinheim, New York, Tokyo, Melbourne, Madras, 1998. P. 93–124.
25. *Bower, D. I.* An Introduction to Polymer Physics. – Cambridge University Press, Cambridge, 2002. P. 162–217.
26. *Parks, T. J., Lynch, L. J., Webster, D. S.* Pyrolysis model of Rundle oil shale from in-situ 1H NMR data // Fuel. 1987. Vol. 66. P. 338–344.
27. *Johnson, R., Kuby, P.* Elementary Statistics. – Thomson Learning, Duxbury 2000. P. 606–649.
28. *Banks, L., Ellis, B.* Broad-line NMR studies of molecular motions in cured epoxy resins // J. Polymer Sci. 1982. Vol. 20. P. 1055–1067.
29. *Aarna, A. J., Alev, M. O.* The i.r. study of the low temperature destruction of oil shale kukersite // Transaction Tallinn Polytech. Inst. 1964. P. 3–14 [in Russian].
30. *Kask, K.* On the bituminization of kukersitic oil shale // Transactions of Tallinn Polytech. Inst. 1955. Vol. A-63. P. 51–64 [in Russian].
31. *Kundel, H., Joonas, R. E., Efimov, B. M., Bitter, L. A.* Differential thermal analysis of the degradation of oil shales // Chemistry of Solid Fuels. 1981. No. 1. P. 65–71 [in Russian].
32. *Duvall, F. E. W., Sohn, H. Y., Pitt, C. H., Bronson, M. C.* Physical behaviour of oil shale at various temperatures and compressive loads: 1. Free thermal expansion // Fuel. 1983. Vol. 62, No. 12. P. 1455–1461.
33. *Haus, Fr., German, J., Junter, G.-A.* Viscosity properties of mineral paraffinic base oils as a key factor in their primary biodegradability // Biodegradation. 2000. Vol. 11. P. 365–369.

34. *Petsch, S. T., Berner, R. A., Eglinton, T. I.* A field study of the chemical weathering of ancient sedimentary organic matter // Organic Geochemistry. 2000. Vol. 31, No. 5. P. 475–487.

35. *Petsch, S. T., Eglinton, T. I., Edwards, K. J.* 14C-Dead living biomass: Evidence for microbial assimilation of ancient organic carbon during shale weathering // Science. 2001. Vol. 292, No. 11. P. 1127–1131.

36. *Krumholz, L. R., Harris, St. H., Suflita, J. M.* Anaerobic microbial growth from components of Cretaceous shales // Geomicrobiology Journal. 2002. Vol. 19. P. 593–602.

37. *Parks, T. J., Lynch, L. J., Webster, D. S., Barret, D.* Molecular properties and thermal transformation of oil shale kerogens from in situ 1H NMR data // Energy & Fuels. 1988. No. 2. P. 185–190.

Presented by A. Raukas
Received January 8, 2005